Supporting Information

Amphiphilic tri- and tetra-block co-polymers combining versatile functionality with facile assembly into cytocompatible nanoparticles

Catherine E. Vasey,[a‡] Amanda K. Pearce,[a‡] Federica Sodano,[b] Robert Cavanagh,[a] Thais Abelha,[a] Valentina Cuzzucoli Crucitti,[c] Akosua B. Anane-Adjei,[a] Marianne Ashford,[d] Paul Gellert,[d] Vincenzo Taresco[a*] and Cameron Alexander.[a*]

‡ authors contributed equally

Table of contents

Figure S14. DLS trace of BOC-deprotected copolymers

Figure S15. Cytotoxicity assays of NPS produced from $mPEG_{5000}$-$(LA)_{50}$-$(tBSC)_{50}$ and its deprotected form.

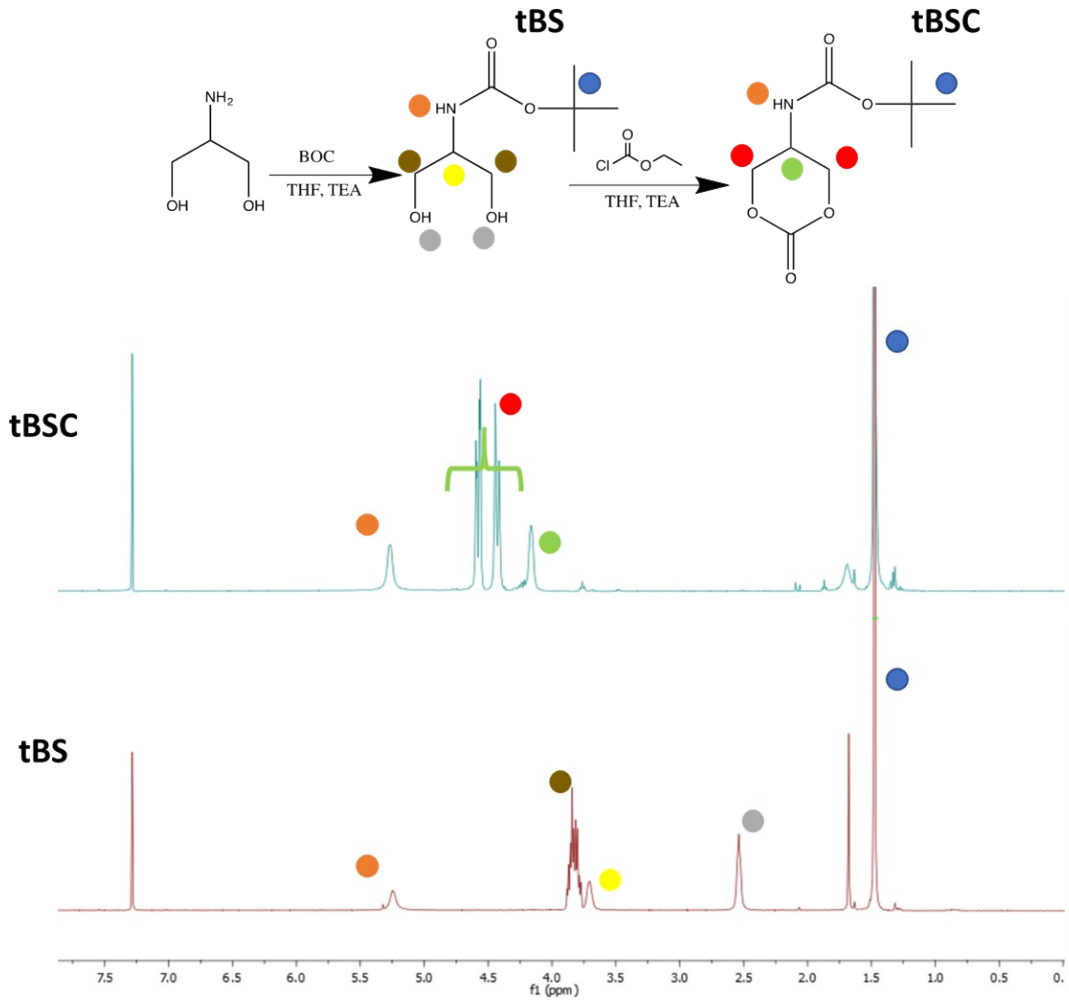

Figure S1. The synthetic scheme for the production of tert-Butyl (2-oxo-1,3-dioxan-5-yl)carbamate (tBSC).

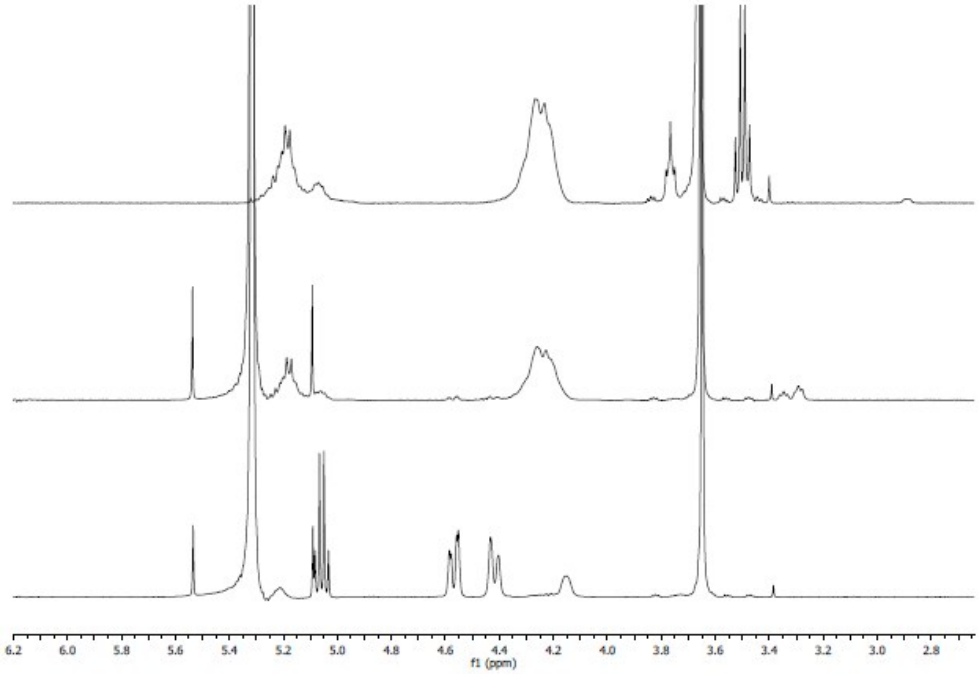

Figure S2. Representative ^{1}H NMR graph (400 MHz, $CDCl_3$) for the ROP of lactide and tBSC initiated by mPEG5000 (P2), showing quantitative polymerisation of both lactide and tBSC after 15 minutes. (A) time = 0 minutes, (B) time = 15 minutes, and (C) post purification.

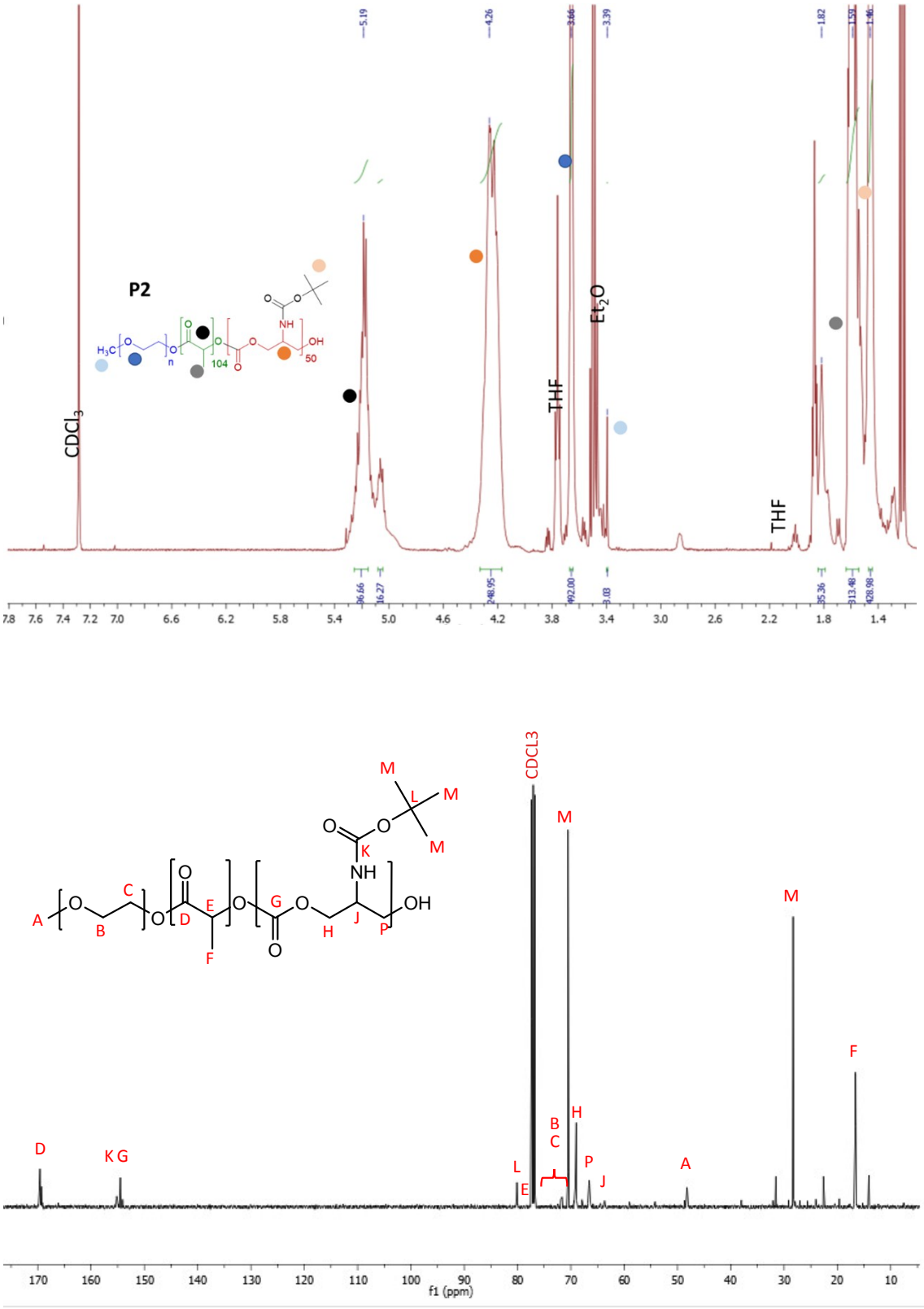

Figure S3. ^{1}H-NMR and ^{13}C-NMR spectrum with integrations of P2 ($mPEG_{5000}$-$(LA)_{50}$-$(tBSC)_{50}$) as model polymer.

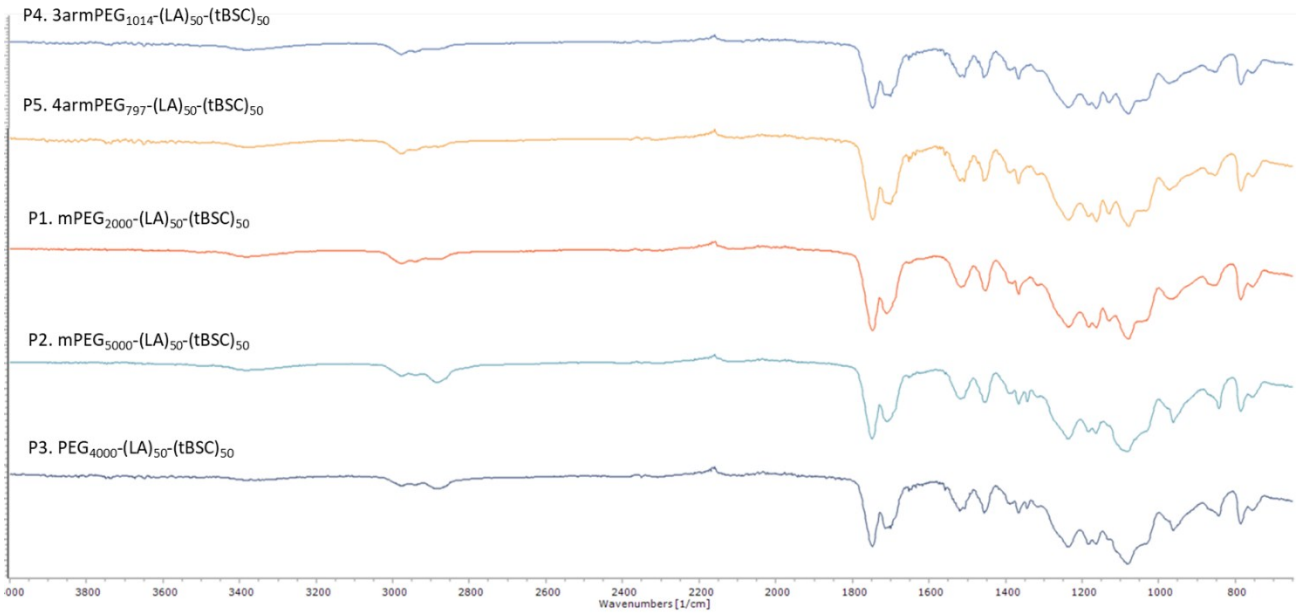

Figure S4. ATR-IR spectra of the five PEGylated ester-carbonate copolymers showing typical peaks of both ester and carbonate functionalities. In particular, C-H stretching in the region between 2900 -2800, $C=O_{ester}$ and $C=O_{carbonate}$ in the region of 1750 - 1680 and the C-O-C bending of the ester and ether (PEG) functionalities at 1100 cm^{-1}.

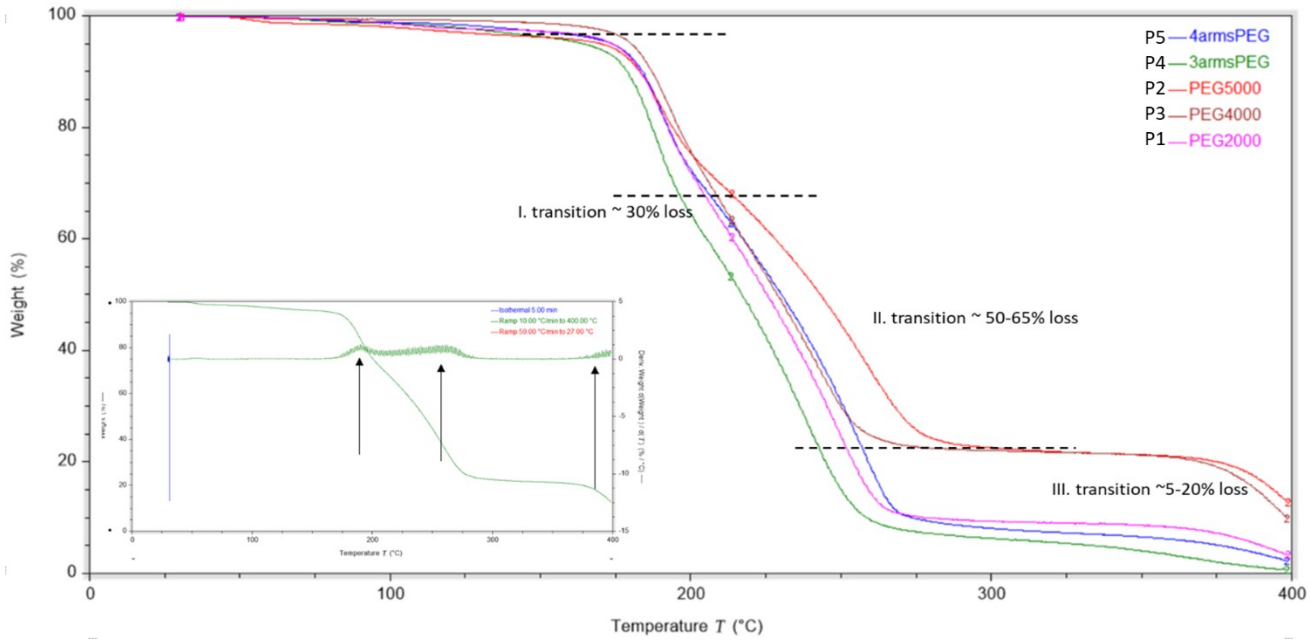

Figure S5. (main) PEGylated copolymers TGA loss profiles. It can be observed three weight loss regions for all the polymers varying according to the length and stability of the PEG chains. (inset) P2 TGA thermogram with derivate-analysis showing three loss weight contributions.

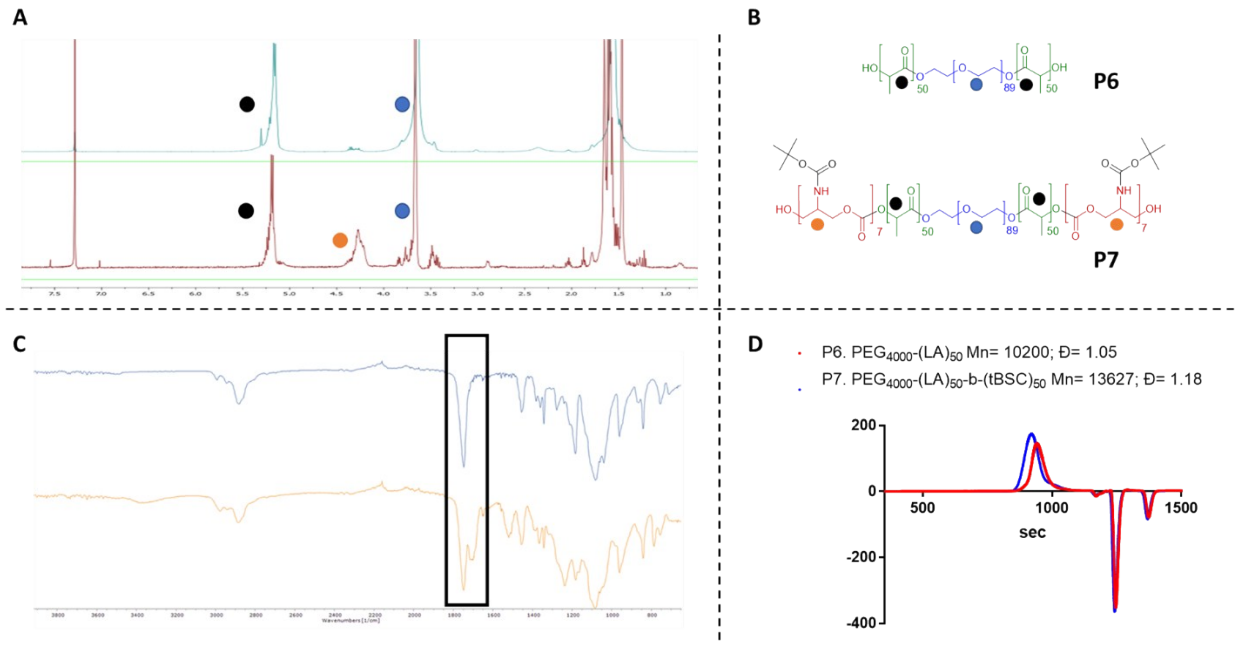

Figure S6. A) ^{1}H-NMR of the PEG_{4000}-initiated LA block (bottom) and tBSC chain extension (top), B) chemical structures of the A-B and A-B-C copolymers, C) stacked ATR-IR spectra of the two copolymers, C=O region highlighted to show the appearance of the carbonate carbonyl peak after successful chain extension, D) GPC traces of the two copolymers, confirming increased molecular weight and monomodal traces.

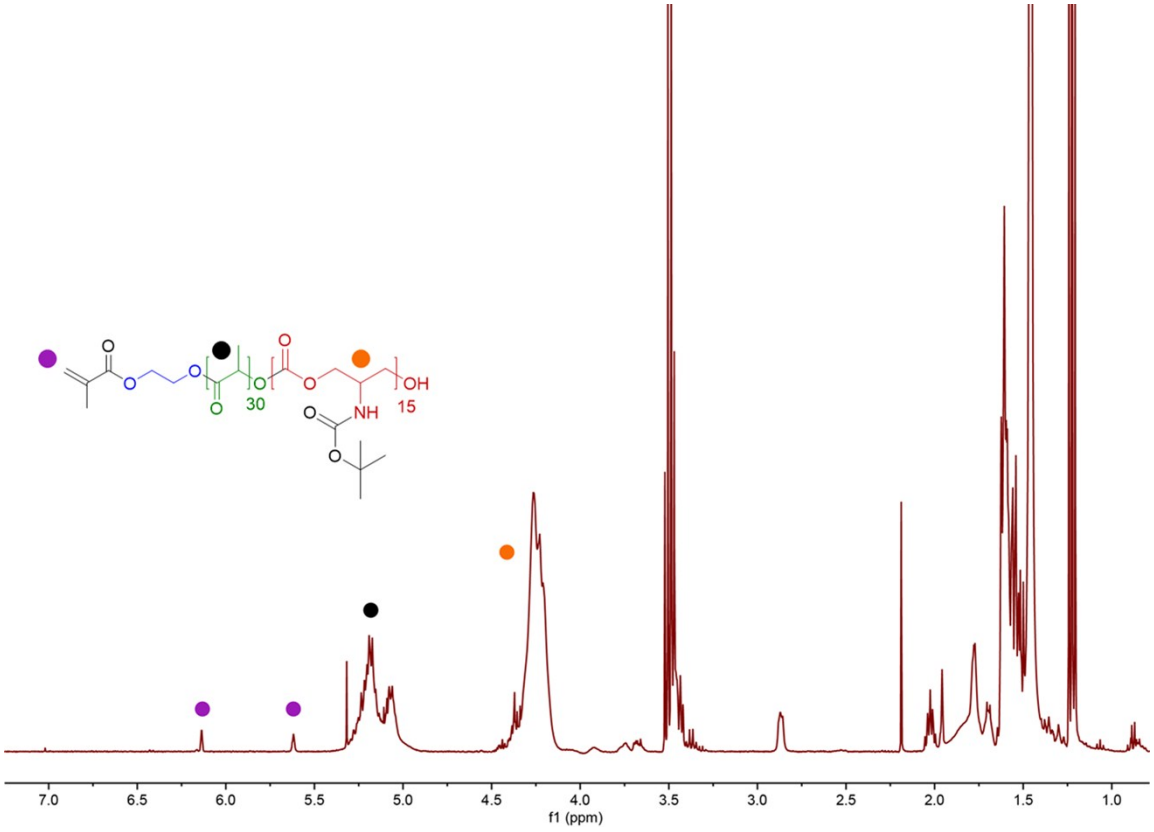

Figure S7. ^{1}H NMR spectra of post purification HEMA-initiated ester-carbonate random macromonomer.

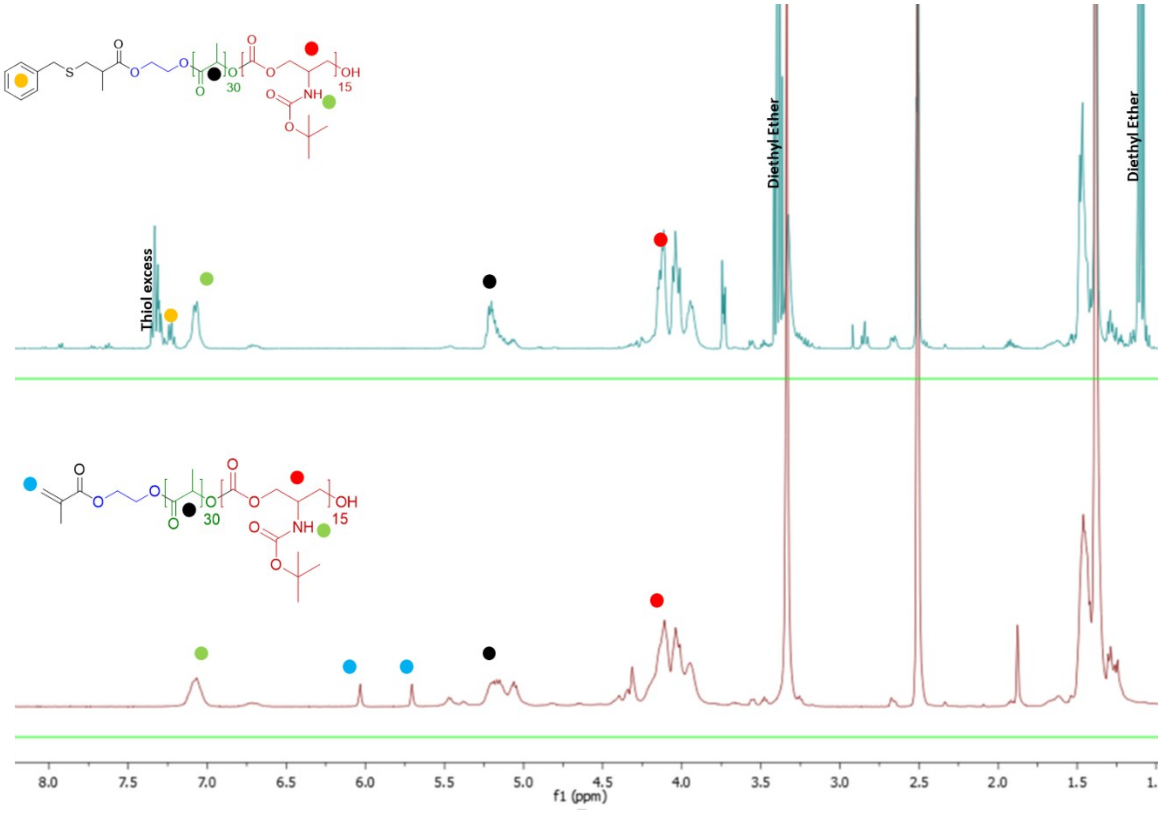

Figure S8. (left) Structure of the thiol-ene click product with starting material on the bottom. (Right) Stacked ^{1}H NMR spectra showing full conversion of vinyl peaks after the click reaction step. Note some excess benzyl mercaptan and precipitation solvents have been highlighted.

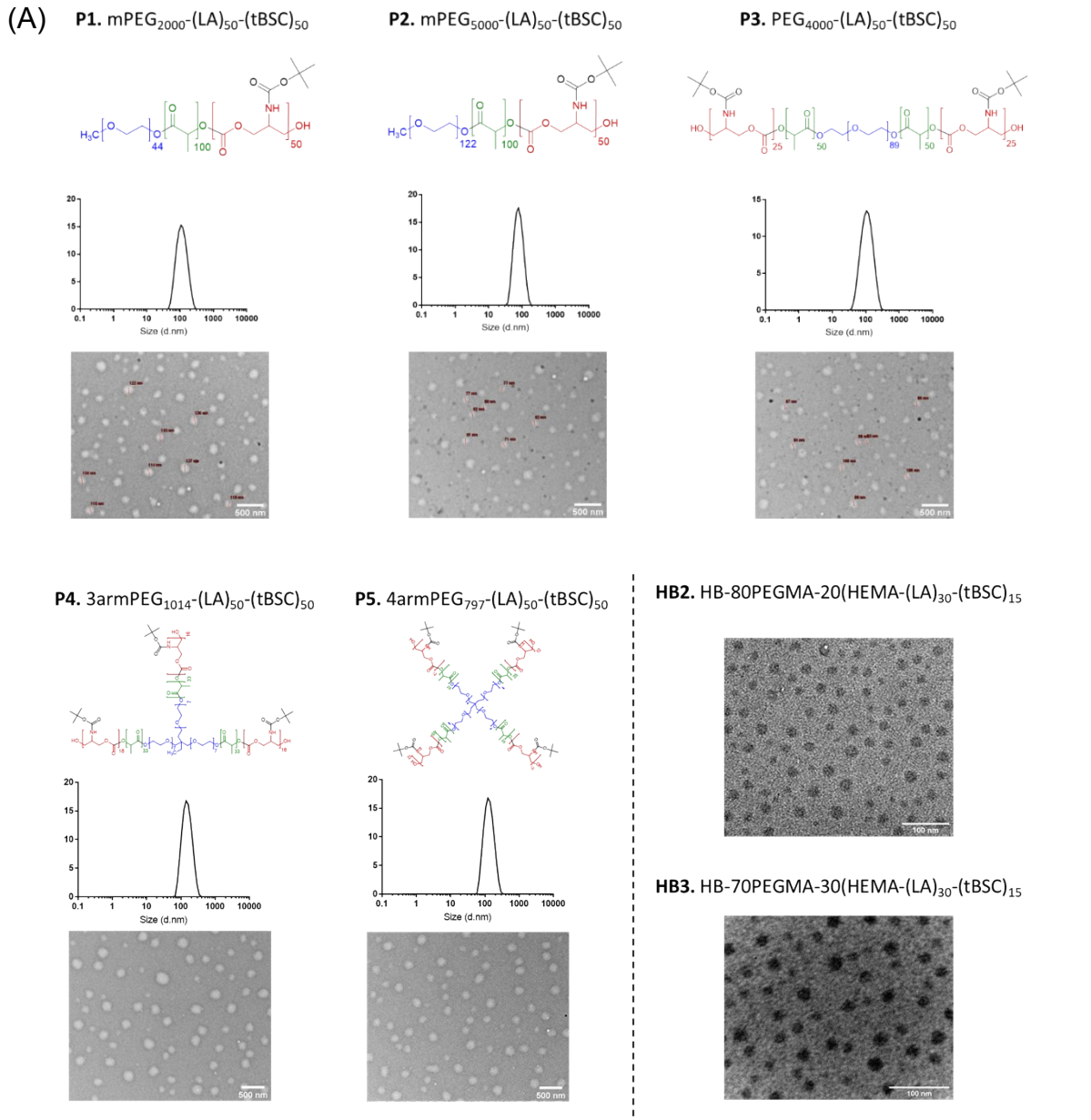

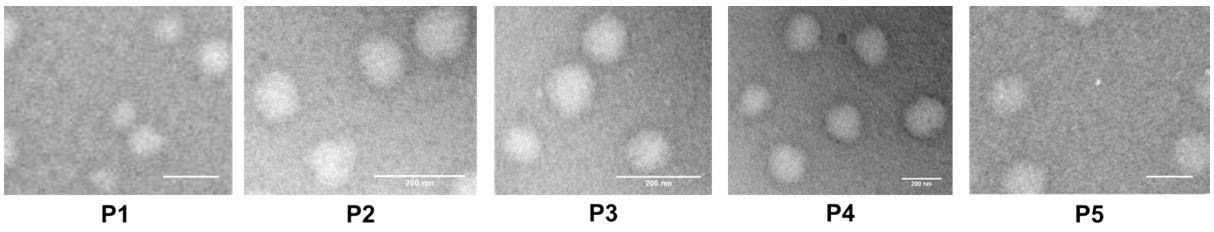

Figure S9. (A) TEM micrographs and DLS traces of NPs produced from PEGylated linear copolymers and TEM micrographs of HB polymers. (B) Magnified TEM micrographs to show approximately spherical structures

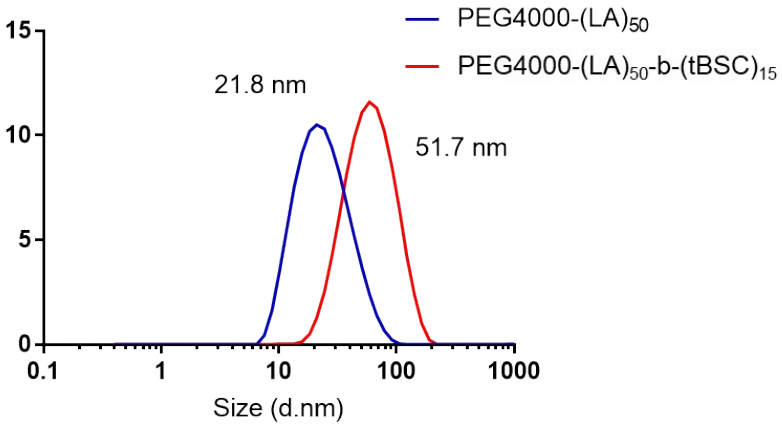

Figure S10. NPs DLS traces formed from P6 (A-B) and P7 (A-B-C) PEG_{4000} initiated copolymers.

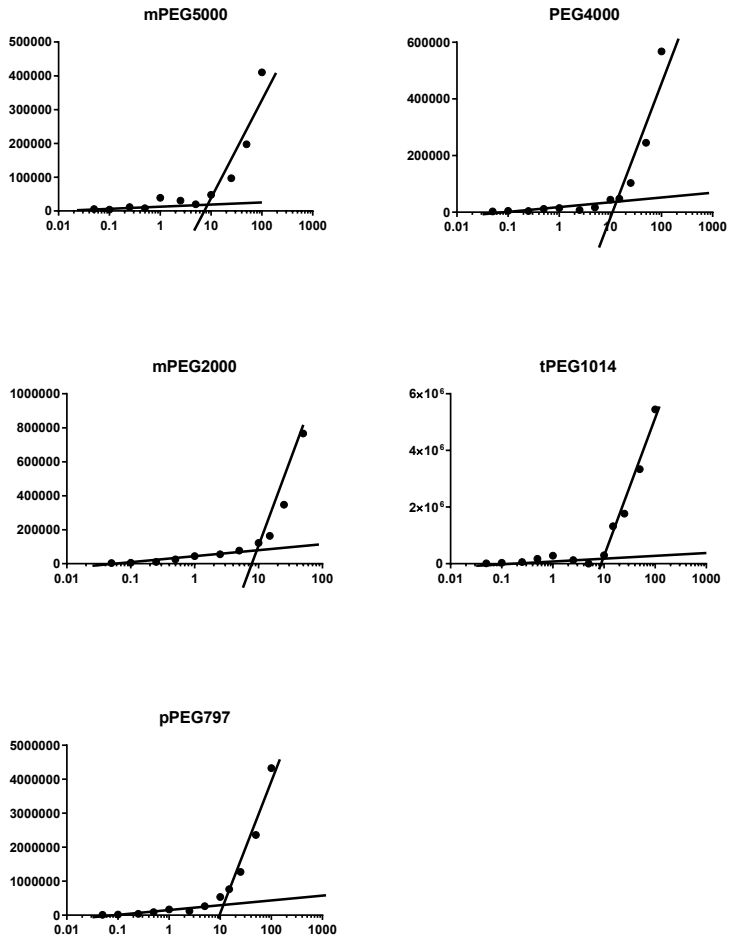

Figure S11. PEGylated copolymers CMC (CAC) graphs of count rate in kcps vs concentration.

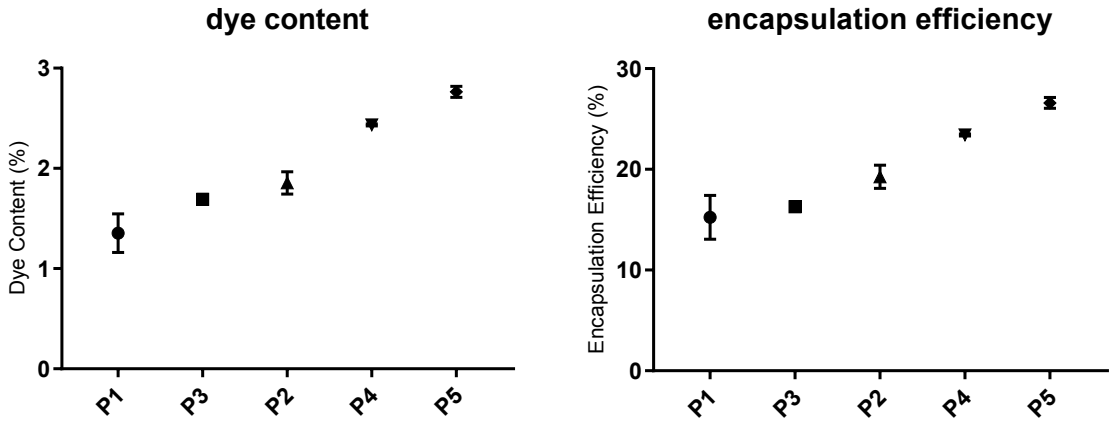

Figure S12. Dye content % and encapsulation efficiency % trends across the PEGylated copolymers.

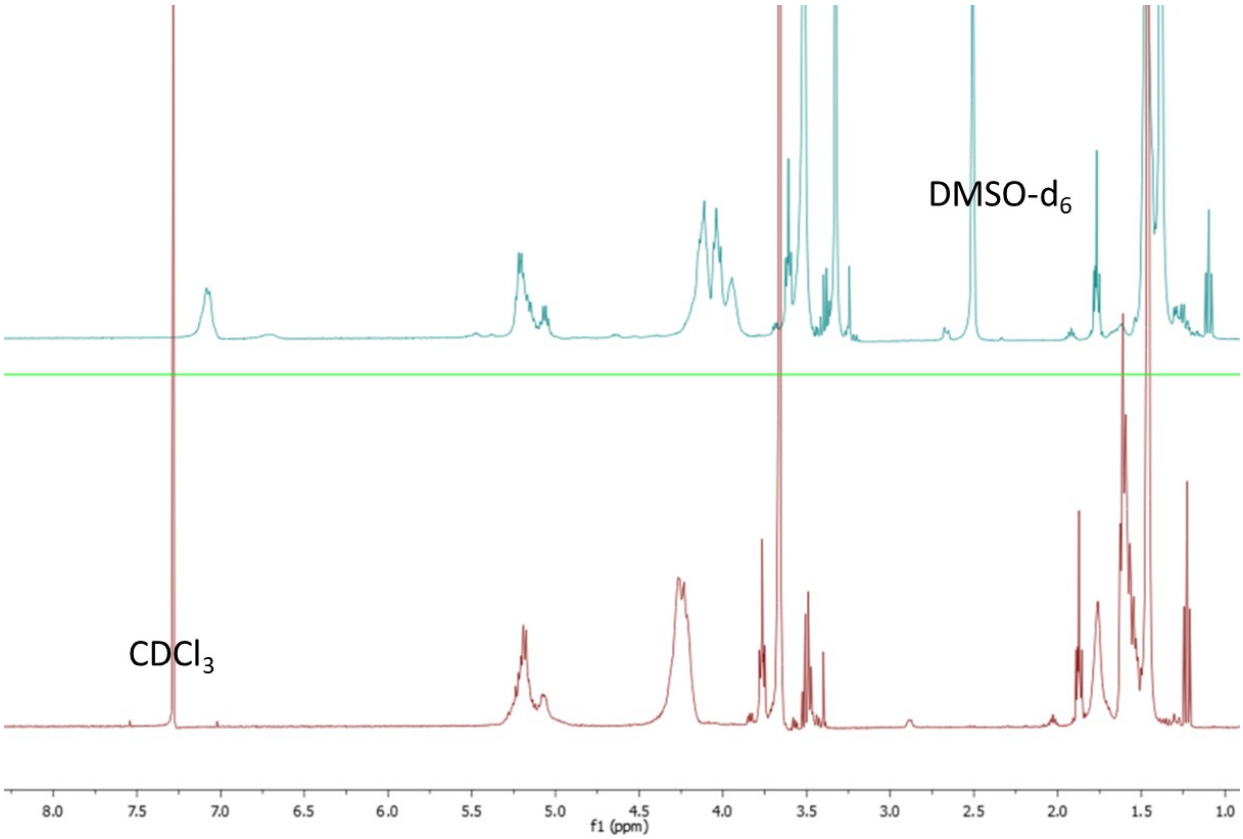

Figure S13. ^{1}H-NMR spectra of P2 copolymer in $CDCl_3$ (bottom) and DMSO-d_6 (top) in order to show peak variations in the two solvents.

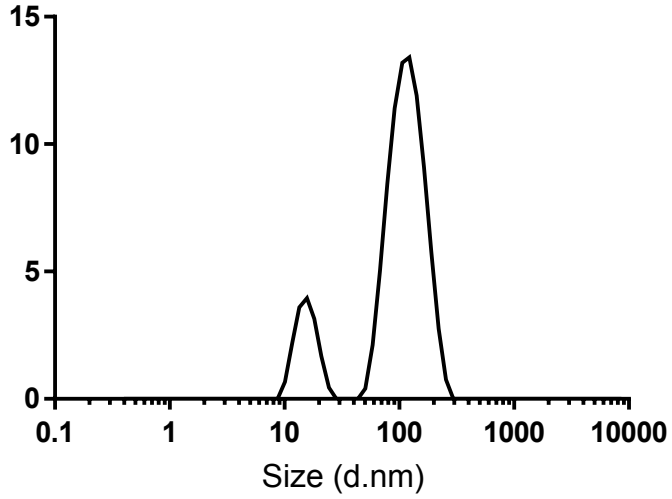

Figure S14. DLS trace of BOC-deprotected $P2^+$ copolymer, showing two peaks underlining the low stability of the charged NPs.

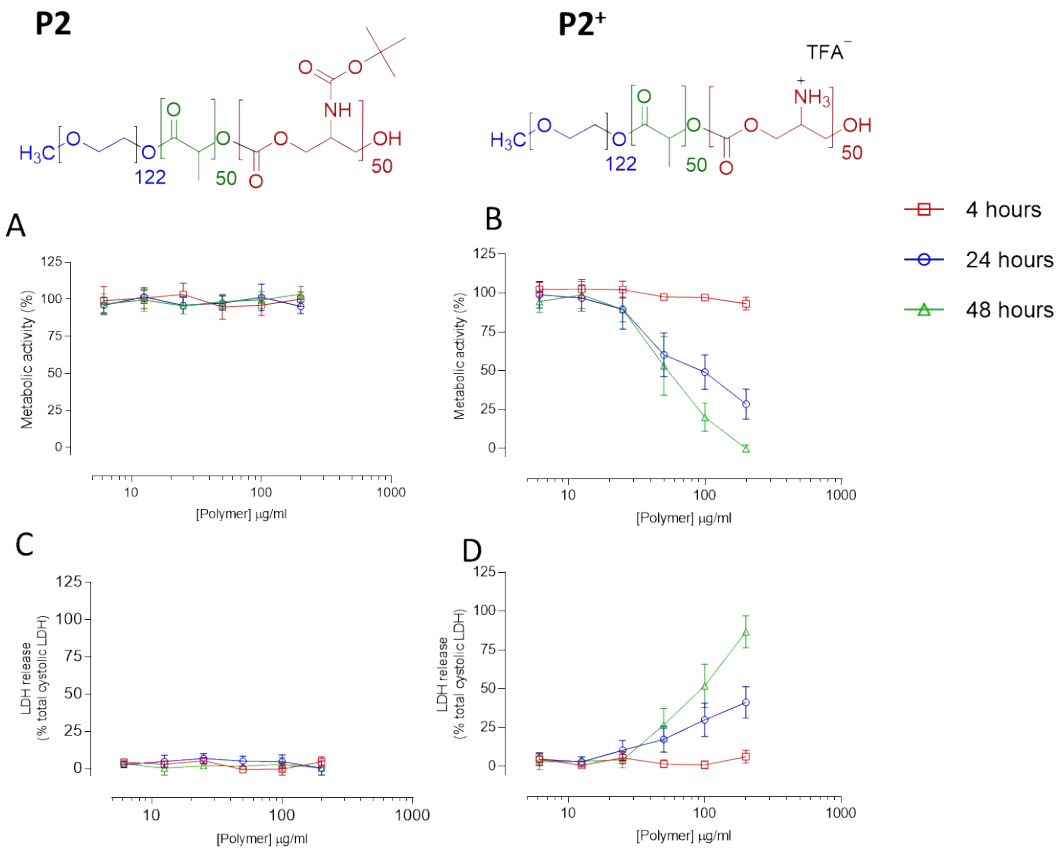

Figure S15. Cellular effects of (A and C) protected (B and D) and de-protected polymer nanoparticles. Metabolic activity (A and B) of MCF7 cells was determined by PrestoBlue assay, and plasma membrane integrity by the LDH release assay (C and D). Data represents mean ± S.D of triplicates coming from three independent experiments.